Defective carbon nanotubes for single-molecule sensing

Zeila Zanolli and J.-C. Charlier
Unité de Physico-Chimie et de Physique des Matriaux (PCPM), European Theoretical Spectroscopy Facility (ETSF), Université catholique de Louvain, Place Croix du Sud 1, 1348 Louvain-la-Neuve, Belgium
(Received 16 June 2009; revised manuscript received 18 September 2009; published 26 October 2009)

The sensing ability of metallic carbon nanotubes toward various gas species (NO_2, NH_3, CO, H_2O, and CO_2) is investigated via *ab initio* calculations and Nonequilibrium Green's Functions technique, focusing on the salient features of the interaction between molecules and oxygenated-defective tubes. As the adsorption/desorption of molecules induces modulations on the electrical conductivity of the tube, the computation of the electron quantum conductance can be used to predict gas detection. Indeed, the analysis of the conductance curve in a small energy range around the Fermi energy reveal that oxygenated-defective nanotubes are sensitive to NO_2, NH_3, CO, and H_2O, but not to CO_2. Molecular selectivity can also be provided by the nature of the charge transfer.

DOI: 10.1103/PhysRevB.80.155447 PACS number(s): 61.46.Fg, 71.15.Mb, 73.22.−f, 73.63.Fg

I. INTRODUCTION

The quest for gas sensors with high sensitivity and selectivity is a research area of growing interest for the numerous applications in the environmental, medical, and industrial fields. Gas sensors based on nanoscale sensing elements are believed to overcome the present limitations of conventional solid-state gas sensors. Indeed, the high surface to volume ratio of one-dimensional (1D) nanostructures greatly enhances the sensitivity and allows for further miniaturization of the devices. Exploiting this idea, sensing devices based on carbon nanotubes (CNT)[1,2] and graphene[3] have been proposed, confirming the outstanding properties of CNT-based sensors such as faster response, higher sensitivity, and selectivity.[4]

The operating principle of CNT-based sensors consists in inducing a modulation on the electrical conductivity of the tube due to the adsorption of gas molecules at the CNT surface, giving rise to the output signal of the nanodevice. However, the microscopic process based on the charge transfer between the adsorbed molecule and the nanotube, affecting its electronic conductance, is still a debated issue. Indeed, earlier first-principles calculations, performed on pristine nanotubes, reveal weak binding energies and small charge transfers from the adsorbed gas, such as O_2,[5] NO_2, and NH_3.[6] These theoretical predictions suggest a poor reactivity from a defect-free CNT surface, thus leading to its insensitivity to molecular exposure in contradiction with experiments.[1,2] Recently, the modulation of the conductance of nitrogen doped CNTs in presence of NH_3 has been studied from first principles.[7] However, as discussed further in this work, the most abundant defect on CNTs walls is the oxygenated vacancy.[1]

In order to understand the observed sensing ability of CNTs at the atomic level, a realistic description of the gas–tube interaction has to be provided. As most materials, CNTs do contain defects[8,9] which strongly affect both their electronic[10] and transport properties.[11,12] These defects (such as vacancies) modify the local electronic-charge distribution, enhancing the tube reactivity at this specific site.[13] In addition, as CNT conductance measurements are known to be strongly affected by air,[1] these highly reactive defects are most probably oxygenated in their stable form. Indeed, even though -OH groups have higher interaction energy with a pristine nanotube as compared to other functional groups containing oxygen,[14] NO_2 molecules have been shown[15] not to bind to the hydroxylated vacancy and to bind, instead, to the oxygenated vacancy. Consequently, the interaction between CNTs containing oxygenated vacancies and various gas species is a realistic model to describe and engineer CNT sensing nanodevices with improved performances and eventually reach the goal of the single-molecule detection limit.[16]

II. COMPUTATIONAL METHODS

In the present work, the ground-state properties of a defective armchair nanotube (containing an oxygenated vacancy) are investigated using the density-functional theory (DFT) (Refs. 17 and 18) as implemented in the SIESTA code.[19] The interaction between the oxygenated-defective tube and various gas species (NO_2, NH_3, CO, CO_2, and H_2O) is predicted by calculating most stable ground-state configurations, binding energies, and charge transfers. Temperature dependence of the adsorption/desorption process is also estimated using quantum molecular dynamics. At last, electronic transport calculations are performed within the nonequilibrium Green's functions (NEGF) (Ref. 20) formalism and using the one-particle Hamiltonian obtained from the DFT calculations as implemented in the SMEAGOL code.[21] Electronic conductances reveal that nanotubes with oxygenated vacancies are particularly sensitive to NO_2, NH_3, CO, and H_2O molecules. Molecular selectivity can be achieved thanks to the different acceptor (NO_2, H_2O)/donor (NH_3, CO) character of the molecules which results in charge transfer of opposite directions, consistently with experimental results.[2,3] Consequently, defective CNTs are potentially good candidates for the selective detection of specific gases with high sensitivity.

Using the outlined DFT formalism, *ab initio* ground-state calculations within the local density approximation[22] are performed to investigate a (5,5) carbon nanotube. Periodic boundary conditions with fixed lateral dimensions are used

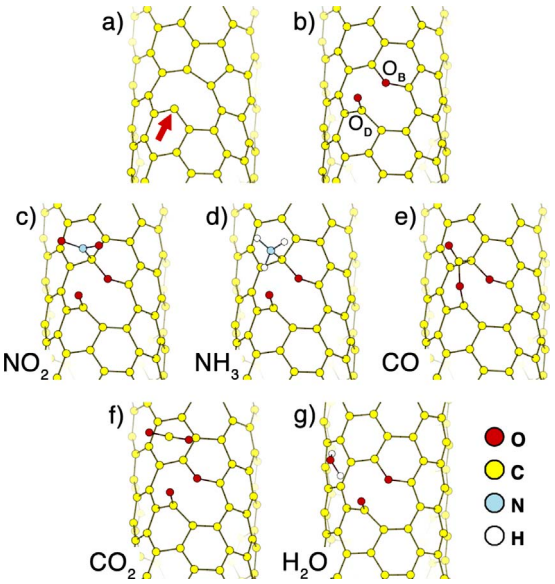

FIG. 1. (Color online) Ball-and-stick models illustrating fully *ab initio* optimized atomic structures of a (5,5) CNT containing a reconstructed monovacancy (a), an oxygenated monovacancy (b), and with various gas molecules adsorbed on the oxygenated-defective site: NO_2 (c), NH_3 (d), CO (e), CO_2 (f), H_2O (g). The color code used to label the atoms is indicated.

to ensure 18 Å of vacuum between the CNTs in neighboring cells. When the vacancy is introduced, a $7\times1\times1$ supercell is considered, leading to a nearest-neighboring defect distance of ~17.5 Å and a defect concentration of ~1%. In order to deal with the large number of atoms in the supercell, numerical atomic orbital basis sets[23] are used to expand the wave-functions, in conjunction with norm-conserving pseudopotentials.[24] The energy levels are populated using a Fermi-Dirac distribution with an electronic temperature of 300 K. The integration over the 1D Brillouin zone is replaced by a summation over a regular grid of 10 k points along the tube axis. The geometry is fully relaxed until the forces on each atom and on the unit cell are less than 0.01 eV/Å and 0.04 eV/Å, respectively.

III. RESULTS AND DISCUSSION

A. Ground-state properties

Within such framework, the interaction between an O_2 molecule and the defective (5,5) tube is studied in order to model realistic nanotubes in air. The monovacancy is known to undergo a Jahn-Teller distortion [Fig. 1(a)]: two of the unsaturated carbon atoms get closer and form a weak covalent bond, inducing a pentagonlike rearrangement.[25] The third unsaturated carbon atom [pointed out by the arrow in Fig. 1(a)] moves radially out of the tube, modifying the initial D_{3h} symmetry of the hexagonal network into the favored C_s symmetry.[26] Approaching the vacancy site with a O_2 molecule directly induces its dissociation. One of the oxygen atoms binds covalently to the dangling carbon atom (dangling oxygen—O_D), creating a double bond with a C-O distance of 1.22 Å. The other O sits in a bridge position (bridging oxygen—O_B) between the two previously bonded carbon atoms [Fig. 1(b)]. Such a chemical process is highly exothermic with a O_2 dissociation/binding energy of ~9.5 eV (Table I). Charge transfer analysis[27,28] between the oxygen atoms and the tube is then performed. Consistently with the high electronegativity of oxygen, both O_D and O_B exhibit an excess charge of $\sim1|e|$, provided by the neighboring carbon atoms ($\sim1|e|$ by the dangling carbon, and $\sim0.45|e|$ by each of the previously bonded carbon). Since the dangling carbon is now linked to O_D by a double bond, the two C atoms connected by O_B are the most reactive sites of the defected zone.

In order to investigate the adsorption of the various gas species on the oxygenated-defective site of the tube surface, a constrained conjugate gradients (CG) (Ref. 29) algorithm is used to minimize the total energy with respect to the molecular trajectory. Starting with different initial configurations allows us to follow various molecular trajectories. For each molecular adsorption, a full *ab initio* CG minimization is performed, leading to the ground-state configurations illustrated in Figs. 1(c)–1(g). Bond lengths and binding energies[30] are summarized in Table I. NO_2, NH_3, and CO are found to be chemisorbed to the defect. The CO binding energy is the highest since it is linked both to a carbon and to an oxygen atom (Table I). On the other hand, bond lengths and binding energies of H_2O and CO_2 indicate that these molecules are physisorbed at the surface of the nanotube. Charge transfer between the tube and the different molecules are subsequently estimated. According to the sign of the charge transfer, NO_2, H_2O, and CO_2 behave as acceptors, while NH_3 and CO as donors (Table I), in agreement with experimental results on semiconducting CNTs (Ref. 2) and on graphene.[3] Hence, the nature of charge transfer turns out to be mainly determined by the molecule and not by the host carbon nanostructure. Since the charge exchanged by phys-

TABLE I. Dissociation and binding energies (E_B,eV), bond lengths (d,Å), and charge transfers (Δq,$|e|$) between the tube and various molecules. Positive (negative) values of Δq denote the acceptor (donor) character of the adsorbed molecule. Atoms are labeled according to Fig. 1.

	O_2	NO_2	NH_3	CO	CO_2	H_2O
E_B	−9.528	−2.026	−1.031	−2.893	−0.180	−0.512
d	1.22 (O_D)	1.58	1.54	1.53 (C)	2.8	3.0
	1.38 (O_B)			1.41 (O_D)		
Δq	1.069 (O_D)	0.347	−0.408	−0.324	0.022	0.048
	1.006 (O_B)					

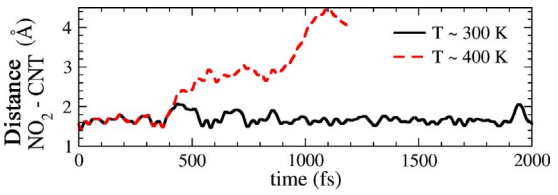

FIG. 2. (Color online) Temperature dependence of the adsorption/desorption process of a NO_2 molecule at the defective site (oxygenated monovacancy) of a (5,5) CNT. At 300 K, the molecule is chemisorbed to the tube, while its desorption is observed around 400 K.

isorbed molecules is quite small, H_2O and CO_2 are not expected to drastically modify the conductance of the tube. On the contrary, chemisorbed molecules (NO_2, NH_3, and CO) exchange a significant fraction of the electron charge and, hence, are expected to have a major effect on the transport properties of the nanotube.

B. Molecular dynamics

In order to check the validity of the CG minimization technique, Born-Oppenheimer quantum molecular dynamics (MD) (Ref. 31) simulation at finite temperature is also used to investigate the adsorption process of a molecule at the nanotube surface. Indeed, conventional CG algorithm is known to trap the system into local energy minima of the potential energy surface, while MD techniques allow the system to overcome potential energy barriers and finally land into the global minimum. Hence, MD simulations are employed to predict the most stable geometry for the molecule-tube system and to study the temperature dependence of the adsorption/desorption process of a NO_2 molecule.

MD calculations are performed using the SIESTA code[19] for a segment of tube 5 unit cells long and saturated with H atoms, which are kept fixed during the simulation. Computational details are identical to those of ground-state calculations, except that only the Γ point is used to sample the Brillouin zone. A time step of 1 fs is used to integrate the Newton equations of motion and a Nosé thermostat[32] with a Nosé mass of 10.0 $Ry \cdot fs^2$ is used to control the temperature of the system.

At first, the oxygenated tube [Fig. 1(b)] is thermalized at 300 K, using a relaxation time of 300 fs. Then, the NO_2 molecule is positioned at a ~6 Å distance from the tube and projected toward the defective site with an initial velocity (5× its average thermal velocity) in order to provide it with enough kinetic energy to overcome the repulsive electron cloud localized on the oxygen atoms. After ~200 fs, the NO_2 molecule reaches the defect and remains chemisorbed at the surface of the tube during ~2 ps of simulation (Fig. 2, full line). If the whole system is cooled down to 0 K, NO_2 remains bound to the tube with an analogous atomic structure as the one illustrated in Fig. 1(c). On the contrary, if the temperature of the whole system is increased to 400 K, NO_2 remains chemisorbed for a few hundreds fs and finally desorbs (Fig. 2, dashed line), qualitatively in agreement with experiment.[33] It should be noticed that the simulated desorption time is extremely short compared to the experimental time scales (of the order of tens or hundreds of minutes) and that the temperature parameter of MD simulations is usually higher than the physical temperature. However, the conclusion that could be drawn from the present MD study is that the switch between adsorption and desorption processes occurs in a very small temperature range of the order of ~100 K.

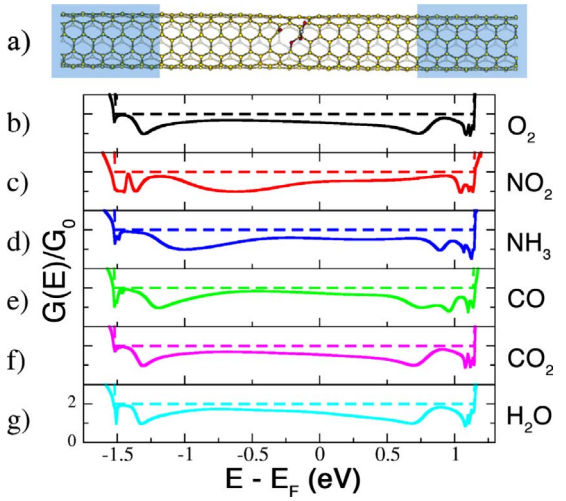

FIG. 3. (Color online) (a) Schematic representation of the model structure used to calculate the electronic conductance: the semi-infinite leads are shaded; the central scattering region contains 13 cells (~260 atoms). Electronic conductance in units of G_0 of a (5,5) CNT with an oxygenated vacancy (b) and in presence of NO_2 (c), NH_3 (d), CO (e), CO_2 (f), H_2O (g) (*core* structures as in Fig. 1). The conductance of pristine (5,5) is indicated with a dashed line.

C. Quantum electron transport

At last, in order to check the gas sensitivity of CNTs, quantum transport calculations are performed, within the NEGF formalism, on a system consisting of a central scattering region and left and right semi-infinite contacts. The contact electrodes (leads) are taken as pristine (5,5) nanotubes, whereas the scattering region consists of 7 "core" cells (including the defective site and the molecule) embedded in 3 leadlike cells on each side, in order to ensure a good screening of the perturbed Hartree potential due to the defect [Fig. 3(a)].

In the absence of an external potential and considering a strong coupling between the scattering region and the leads, the NEGF formalism reduces to the Landauer-Büttiker description for equilibrium transport,[34] where the electron conductance $G(E)$ and the transmission function $T(E)$ at a given energy E are related by $G(E)=T(E)G_0$, where $G_0=2e^2/h$ is the quantum of conductance. Within such an approach, the ballistic conductance of a perfect system is proportional to the number of conducting channels, that is, the number of bands at a given energy. Indeed, the band structure of armchair CNTs is characterized by the crossing of two energy bands in the vicinity of E_F, inducing a quantum conductance of $2G_0$ in the corresponding energy region (Fig. 3, dashed

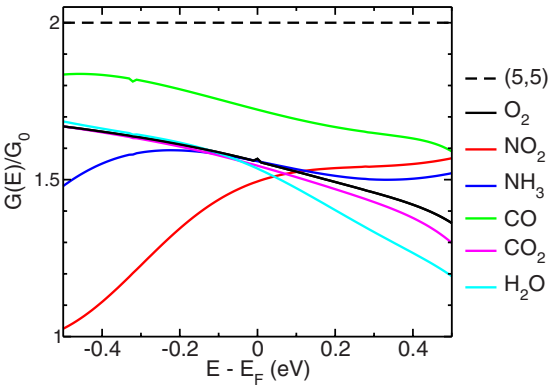

FIG. 4. (Color online) Quantum electron conductances (in units of G_0) of the pristine (5,5) tube (dashed line), of the defected-oxygenated tube (black line), and with adsorbed gas molecules at the defect site (NO_2, NH_3, CO, CO_2, H_2O—colored lines).

line). However, the conductance of an imperfect system is lowered, since the defect acts as a scattering center thus imposing the reflection of electronic waves.[35,36] Figure 3(b) illustrates that oxygenated monovacancy induce some dips in the conductance curve of the (5,5) tube. The corresponding conductance drops to $\sim 1G_0$, that is, one transmission channel is completely suppressed. Two of these dips, positioned at ~ 1.3 eV below and ~ 0.74 eV above E_F, correspond to localized (quasibound) states in the DOS, as already observed for the nonoxygenated vacancy.[36–38]

A molecule, chemisorbed at the defective site of a CNT, generates a shift in energy of these localized states in the DOS, hence, relocating the corresponding dips in the conductance [Figs. 3(c)–3(e)]. A wider dip in the vicinity of E_F arises when either NO_2 or NH_3 is adsorbed at the CNT surface [Figs. 3(c) and 3(d)], indicating a larger mixing of the molecular states with those of the tube. Both the position and the width of these dips in the transmission function can be seen as a signature of the presence of a specific gas at the CNT surface. Indeed, quantum conductance can be measured by applying a voltage through the nanotube and sampling the conductance curve at the corresponding energy. However, detecting the shift of the −1.3 eV dip in the conductance related to the defected-oxygenated tube to its new molecular-dependent locations [−0.65 eV (NO_2), −1 eV (NH_3), and −1.24 eV (CO), respectively] might require high applied voltages, thus inducing possible desorption of the molecule from the CNT due to overheating.

Nevertheless, some specific properties of the conductance curve around the Fermi energy, such as its slope and/or its integral over a small energy range, could be accurately measured experimentally by applying lower voltages thus providing information at the charge transport level on the molecular adsorption. For instance, the percentage change in the conductance at E_F with respect to the bare defected-oxygenated tube can reveal the presence of CO (10% change), NO_2 (4.6%), and even H_2O (2.0%) (see Fig. 4 and Table II). However, the eventual binding of NH_3 and CO_2 cannot be inferred only by looking at the conductance at E_F. On the other hand, additional indications on gas adsorption can be extracted by comparing the integral of the conductance over a specific energy range (see Table II). For instance, NO_2, CO, and NH_3 (but not CO_2 or water) can be detected by integrating the transmission curve in the [−0.5,0.0] eV range. Instead, CO, H_2O, and, to a minor extent, NO_2 and NH_3 can be detected by integrating in the [0.0,0.5] eV range. Still, CO_2 seems to be difficult to detect, even by integrating in the [0.0,0.5] eV range. Finally, it can be noticed that NO_2 adsorption induces the slope of the conductance at E_F to switch from a negative value to a positive one, as illustrated in Fig. 4. Such a slope modification would allow to distinguish selectively adsorption of NO_2 from adsorption of NH_3, CO, CO_2, and H_2O (where a negative slope is conserved).

TABLE II. Percentage of changes in the quantum conductance at the Fermi energy $[\Delta T(E_F)]$ and in the energy intervals $[-0.5,0.0]$ eV $[\Delta T^- = \Delta\int_{-0.5}^{0} T(E)dE]$ and $[0.0,0.5]$ eV $[\Delta T^+ = \Delta\int_{0}^{0.5} T(E)dE]$ for various molecules adsorbed on the defected-oxygenated (5,5) CNT. The changes are calculated with respect to the bare defected-oxygenated tube.

	$\Delta T(E_F)$	ΔT^-	ΔT^+
NO_2	4.6%	21.3%	−4.4%
NH_3	0.5%	3.2%	−3.0%
CO	10.0%	−10.8%	−12.8%
CO_2	1.4%	0.4%	2.0%
H_2O	2.0%	−0.2%	7.1%

Note that these quantitative theoretical predictions may depend on the nanotube diameter and on the nature of the defect. Consequently, comparison with experimental measurements should be performed with care, and theoretical models should be adjusted accordingly. In addition, a realistic model of the sensing ability of a CNT should also take into account the combined effect of the adsorption of different molecules on different kind of defect sites, analogously to the study presented in Ref. 7. Nevertheless, our electronic transport calculations suggest that each molecule affects the conductance of the tube in a specific way and that these conductance changes could actually be measured experimentally by planning specific measurements to analyze the conductance curve around E_F. The predicted sensitivity of metallic CNTs toward NO_2, NH_3, CO, and H_2O molecules is consistent with recent experimental data.[2–4] The case of H_2O is especially interesting since its possible detection can only be inferred by analyzing the conductance curve and not from *ab initio* binding energies and charge transfer considerations. On the contrary, the detection of CO_2 is quite difficult to achieve, still in agreement with sensing experiments performed on graphene.[3]

IV. CONCLUSION

In conclusion, the potential use of carbon nanotubes as sensitive elements for gas detection has been investigated using first principles. The structural, electronic, and quantum transport properties of realistic CNTs, namely, tubes containing oxygenated defects, have been predicted and analogies

with sensing experiments on graphene and semiconducting CNTs have been pointed out. The presence of an oxygenated vacancy at the CNT surface results in an overall increase in interaction strength (binding energies, charge transfer) between the tube and the various molecules. Chemisorbed molecules (NO_2, NH_3, and CO) exchange a significant fraction of electronic charge with the tube, thus modifying in a specific way the tube conductance and, hence, are more likely to be detected. Indeed, the analysis of the conductance curve around E_F shows that defective CNTs are found to be sensitive to NO_2, NH_3, and CO. In addition, the weakly bound H_2O could be detected by measuring conductance changes in a small energy range above the Fermi energy. The interaction of CO_2 with the tube is, instead, so weak that this gas could hardly be detected. However, to associate the change in conductance to the adsorption of a specific molecule a specific set of measurements has to be designed. Finally, the nature of the charge transfer can be exploited to improve selectivity of the detection.

The temperature dependence of both the adsorption and desorption process of NO_2 confirms that the CNT-based sensor can be used at room temperature, and assess the reuse of the sensor after heating it up at higher temperature. At last, our results demonstrate that an in depth understanding of the nature of the molecule-nanotube interaction is required to accurately interpret experiments, but also to obtain functional electronic nanodevices.

ACKNOWLEDGMENTS

J.-C.C. acknowledges financial support from the F.R.S.-FNRS of Belgium. Parts of this work are directly connected to the Nano2Hybrids project (EC-STREP-033311), to the Belgian Program on Interuniversity Attraction Poles (PAI6) on "Quantum Effects in Clusters and Nanowires," and to the ARC sponsored by the Communauté Française de Belgique. Computational resources have been provided by the Université catholique de Louvain: all the numerical simulations have been performed on the LEMAITRE and GREEN computers of the CISM.

[1] P. G. Collins, K. Bradley, M. Ishigami, and A. Zettl, Science **287**, 1801 (2000).
[2] J. Kong, N. R. Franklin, C. W. Zhou, M. G. Chapline, S. Peng, K. J. Cho, and H. J. Dai, Science **287**, 622 (2000).
[3] F. Schedin, A. K. Geim, S. V. Morozov, E. W. Hill, P. Blake, M. I. Katsnelson, and K. S. Novoselov, Nature Mater. **6**, 652 (2007).
[4] T. Zhang, S. Mubeen, N. V. Myung, and M. A. Deshusses, Nanotechnology **19**, 332001 (2008).
[5] S.-H. Jhi, S. G. Louie, and M. L. Cohen, Phys. Rev. Lett. **85**, 1710 (2000).
[6] H. Chang, J. D. Lee, S. M. Lee, and Y. H. Lee, Appl. Phys. Lett. **79**, 3863 (2001).
[7] A. R. Rocha, M. Rossi, A. Fazzio, and A. J. R. da Silva, Phys. Rev. Lett. **100**, 176803 (2008).
[8] A. Hashimoto, K. Suenaga, A. Gloter, K. Urita, and S. Iijima, Nature (London) **430**, 870 (2004).
[9] K. Suenaga, H. Wakabayashi, M. Koshino, Y. Sato, K. Urita, and S. Iijima, Nat. Nanotechnol. **2**, 358 (2007).
[10] J.-C. Charlier, Acc. Chem. Res. **35**, 1063 (2002).
[11] C. Gómez-Navarro, P. J. De Pablo, J. Gómez-Herrero, B. Biel, F. J. Garcia-Vidal, A. Rubio, and F. Flores, Nature Mater. **4**, 534 (2005).
[12] J.-C. Charlier, X. Blase, and S. Roche, Rev. Mod. Phys. **79**, 677 (2007).
[13] L. Valentini, F. Mercuri, I. Armentano, C. Cantalini, S. Picozzi, L. Lozzi, S. Santucci, A. Sgamellotti, and J. M. Kenny, Chem. Phys. Lett. **387**, 356 (2004).
[14] A. Felten, C. Bittencourt, J.-J. Pireaux, G. Van Lier, and J.-C. Charlier, J. Appl. Phys. **98**, 074308 (2005).
[15] R. Ionescu, E. H. Espinosa, E. Sotter, E. Llobet, X. Vilanova, X. Correig, A. Felten, C. Bittencourt, G. Van Lier, J.-C. Charlier, and J. J. Pireaux, Sens. Actuators B Chem. **113**, 36 (2006).
[16] B. R. Goldsmith, J. G. Coroneus, A. A. Kane, G. A. Weiss, and P. G. Collins, Nano Lett. **8**, 189 (2008).
[17] P. Hohenberg and W. Kohn, Phys. Rev. **136**, B864 (1964).
[18] W. Kohn and L. J. Sham, Phys. Rev. **140**, A1133 (1965).
[19] J. M. Soler, E. Artacho, J. Gale, D. A. Garcia, J. Junquera, P. Ordejón, and D. Sánchez-Portal, J. Phys.: Condens. Matter **14**, 2745 (2002).
[20] S. Datta, *Electronic Transport in Mesoscopic Systems* (Cambridge University Press, Cambridge, 1995).
[21] A. R. Rocha, V. M. Garcia-Suárez, S. Bailey, C. Lambert, J. Ferrer, and S. Sanvito, Phys. Rev. B **73**, 085414 (2006).
[22] Spin-polarized calculations have also been performed, finding that the defected-oxygenated tube and the defected-oxygenated tube with adsorbed gas molecules are not spin polarized.
[23] A numerical atomic orbital basis set of quality double ζ plus one polarization is used for all the atoms: with an energy shift of 272 meV for C and N, and the O and H orbital basis sets optimized for H_2O [J. Junquera *et al.*, Phys. Rev. B **64**, 235111 (2001)]. The real-space grid cutoff is 300 Ry.
[24] N. Troullier and J. L. Martins, Phys. Rev. B **43**, 1993 (1991).
[25] P. M. Ajayan, V. Ravikumar, and J.-C. Charlier, Phys. Rev. Lett. **81**, 1437 (1998).
[26] H. Amara, S. Latil, V. Meunier, P. Lambin, and J.-C. Charlier, Phys. Rev. B **76**, 115423 (2007).
[27] R. F. W. Bader, *Atoms in Molecules—A Quantum Theory* (Oxford University Press, Oxford, 1990).
[28] E. Sanville, S. D. Kenny, R. Smith, and G. Henkelman, J. Comput. Chem. **28**, 899 (2007).
[29] M. P. Teter, M. C. Payne, and D. C. Allan, Phys. Rev. B **40**, 12255 (1989).
[30] Note that all binding energies are calculated including the corrections to the basis set superposition error: S. F. Boys and F. Bernardi, Mol. Phys. **19**, 553 (1970).
[31] P. Bendt and A. Zunger, Phys. Rev. Lett. **50**, 1684 (1983).
[32] S. Nosé, Prog. Theor. Phys. **103**, 1 (1991).

[33] R. Q. Long and R. T. Yang, Ind. Eng. Chem. Res. **40**, 4288 (2001).
[34] M. Büttiker, Y. Imry, R. Landauer, and S. Pinhas, Phys. Rev. B **31**, 6207 (1985).
[35] L. Chico, L. X. Benedict, S. G. Louie, and M. L. Cohen, Phys. Rev. B **54**, 2600 (1996).
[36] H. J. Choi, J. Ihm, S. G. Louie, and M. L. Cohen, Phys. Rev. Lett. **84**, 2917 (2000).
[37] Y. W. Son, M. L. Cohen, and S. G. Louie, Nano Lett. **7**, 3518 (2007).
[38] A. R. Rocha, J. E. Padilha, A. Fazzio, and A. J. R. da Silva, Phys. Rev. B **77**, 153406 (2008).